

University of Groningen

Application of free energy expansions to mesoscopic dynamics of copolymer melts using a Gaussian chain molecular model

Maurits, N. M.; Fraaije, J. G. E. M.

Published in:
Journal of Chemical Physics

DOI:
[10.1063/1.473670](https://doi.org/10.1063/1.473670)

IMPORTANT NOTE: You are advised to consult the publisher's version (publisher's PDF) if you wish to cite from it. Please check the document version below.

Document Version
Publisher's PDF, also known as Version of record

Publication date:
1997

[Link to publication in University of Groningen/UMCG research database](#)

Citation for published version (APA):

Maurits, N. M., & Fraaije, J. G. E. M. (1997). Application of free energy expansions to mesoscopic dynamics of copolymer melts using a Gaussian chain molecular model. *Journal of Chemical Physics*, 106(16), 6730-6743. <https://doi.org/10.1063/1.473670>

Copyright

Other than for strictly personal use, it is not permitted to download or to forward/distribute the text or part of it without the consent of the author(s) and/or copyright holder(s), unless the work is under an open content license (like Creative Commons).

Take-down policy

If you believe that this document breaches copyright please contact us providing details, and we will remove access to the work immediately and investigate your claim.

Downloaded from the University of Groningen/UMCG research database (Pure): <http://www.rug.nl/research/portal>. For technical reasons the number of authors shown on this cover page is limited to 10 maximum.

Application of free energy expansions to mesoscopic dynamics of copolymer melts using a Gaussian chain molecular model

N. M. Maurits, and J. G. E. M. Fraaije

Citation: *J. Chem. Phys.* **106**, 6730 (1997); doi: 10.1063/1.473670

View online: <https://doi.org/10.1063/1.473670>

View Table of Contents: <http://aip.scitation.org/toc/jcp/106/16>

Published by the [American Institute of Physics](#)

Articles you may be interested in

[Dynamic density functional theory for microphase separation kinetics of block copolymer melts](#)

The Journal of Chemical Physics **99**, 9202 (1993); 10.1063/1.465536

[The dynamic mean-field density functional method and its application to the mesoscopic dynamics of quenched block copolymer melts](#)

The Journal of Chemical Physics **106**, 4260 (1997); 10.1063/1.473129

[Mesoscopic dynamics of copolymer melts: From density dynamics to external potential dynamics using nonlocal kinetic coupling](#)

The Journal of Chemical Physics **107**, 5879 (1997); 10.1063/1.474313

[Dynamic simulation of diblock copolymer microphase separation](#)

The Journal of Chemical Physics **108**, 8713 (1998); 10.1063/1.476300

[Dynamics of surface directed mesophase formation in block copolymer melts](#)

The Journal of Chemical Physics **110**, 2250 (1999); 10.1063/1.477837

[Perspective: Dissipative particle dynamics](#)

The Journal of Chemical Physics **146**, 150901 (2017); 10.1063/1.4979514

PHYSICS TODAY

WHITEPAPERS

ADVANCED LIGHT CURE ADHESIVES

Take a closer look at what these environmentally friendly adhesive systems can do

READ NOW

PRESENTED BY
 **MASTERBOND**
ADHESIVES | SEALANTS | COATINGS

Application of free energy expansions to mesoscopic dynamics of copolymer melts using a Gaussian chain molecular model

N. M. Maurits and J. G. E. M. Fraaije

Groningen Biomolecular Sciences and Biotechnology Institute, Bioson Research Institute, University of Groningen, Department of Biophysical Chemistry, Nijenborgh 4, 9747 AG Groningen, The Netherlands

(Received 3 June 1996; accepted 16 January 1997)

The present paper deals with some mathematical aspects of generalized time-dependent Ginzburg–Landau theories for the numerical simulation of mesoscale phase separation kinetics of copolymer melts. We shortly discuss the underlying theory and introduce an expansion of the external potential, to be used in the dynamics algorithm, which is similar to free-energy expansions. This expansion is valid for both compressible and incompressible multicomponent copolymer melts using a Gaussian chain model. The expansion is similar to the well-known random phase approximation (RPA) but differs in some important aspects. Also, the application of RPA like free energy expansions to dynamics is new. Our derivation leads to simple expressions for the vertex coefficients, which enables us to numerically calculate their full wave vector dependence, without assuming an ordered morphology. We find that our fourth-order vertex is negative for some wave vectors which has important consequences for the *simulation* of mesoscopic dynamics. We propose a fitting procedure for the vertex coefficients to overcome the computationally expensive calculation of the linear and bilinear expansion terms in the expansion. This procedure provides analytically derived parameters for a gradient free energy expansion, which allows for a whole new class of phase-separation models to be defined. © 1997 American Institute of Physics. [S0021-9606(97)50216-9]

I. INTRODUCTION

A. General

The present paper deals with some important mathematical aspects of generalized time-dependent Ginzburg–Landau theories for the numerical simulation of mesoscale phase separation kinetics of copolymer melts. A few recent references of groups working in this field are Refs. 1–3; two modern reviews of coarse grained time-dependent Ginzburg–Landau and related models are in Refs. 4 and 5. The prototype of these types of coarse-grained models is an M -component functional Langevin equation for conserved order parameters of the following general form:⁶

$$\begin{aligned} \frac{\partial \rho_I(\mathbf{r})}{\partial t} &= \sum_{J=1}^M \int_V \mathcal{D}_{IJ}(\mathbf{r}, \mathbf{r}_1) \mu_J(\mathbf{r}_1) d\mathbf{r}_1 \\ &\quad - \beta^{-1} \sum_{J=1}^M \int_V \frac{\delta \mathcal{D}_{IJ}(\mathbf{r}, \mathbf{r}_1)}{\delta \rho_J(\mathbf{r}_1)} d\mathbf{r}_1 + \eta_I(\mathbf{r}, t), \\ \mathcal{D}_{IJ}(\mathbf{r}, \mathbf{r}_1) &= \nabla_{\mathbf{r}} \cdot \Lambda_{IJ}(\mathbf{r}, \mathbf{r}_1) \nabla_{\mathbf{r}_1}, \end{aligned} \quad (1)$$

with particle concentration fields $\rho_I(\mathbf{r}) (I=1, \dots, M)$, transport coefficients Λ_{IJ} , intrinsic chemical potentials $\mu_I \equiv \delta F / \delta \rho_I(\mathbf{r})$ (F is the free energy), $\beta^{-1} = k_B T$ and noise fields $\eta_I(\mathbf{r}, t)$. The noise has a Gaussian distribution with moments dictated by a fluctuation-dissipation theorem.^{6–8}

In the review papers and references one can find ample examples of computer simulations of time-dependent Ginzburg–Landau models for two-component incompressible liquids with linear transport coefficients and simple fourth-order phenomenological expansion models for the free energy.

It is important to realize how our approach differs from the usual phenomenological expansion methods; to this end, we will briefly recapitulate popular expansion models. Recently, Seul and Andelman presented an elegant overview of fourth-order phenomenological free energy expansions, summarizing a large variety of pattern formation models for many different physical systems.⁹ These expansions contain only the bare ingredients necessary to describe the basic physics of competing interactions. Restricted to the special case of incompressible copolymer melts, an example of such a simplified fourth-order expansion for the free energy reads

$$\begin{aligned} F[\phi] &= \int_V \left[\frac{1}{2} \tau \phi^2 + \frac{1}{4} u \phi^4 + \frac{1}{2} b |\nabla \phi|^2 \right. \\ &\quad \left. - \frac{\mu^2}{2} \int_V \frac{\phi(\mathbf{r}) \phi(\mathbf{r}_1)}{|\mathbf{r} - \mathbf{r}_1|} d\mathbf{r}_1 \right] d\mathbf{r}, \end{aligned} \quad (2)$$

where $\phi \equiv \rho_A - \rho_B$ is the order parameter and τ, u, b , and μ are phenomenological coefficients. The expansion consists of a fourth-order (Landau) expansion in ϕ , a Cahn–Hilliard penalty on spatial gradients and a term which introduces effective long-range interactions due to the connectivity of the copolymer blocks. Depending on the choice of the parameters, this expansion may predict the geometry of various kinds of complex patterns in copolymer melts. Some time ago, Oono and Shiwa introduced a time-dependent Ginzburg–Landau model to calculate the formation of patterns, using essentially the same free energy expansion

$$\frac{\partial \phi}{\partial t} = L \nabla^2 \frac{\delta F}{\delta \phi} = L \nabla^2 (\tau \phi + u \phi^3 - b \nabla^2 \phi) - \mu^2 \phi. \quad (3)$$

This model has been thoroughly studied, both theoretically^{10,11} and numerically.^{12–14} Since the right-hand side of Eq. (3) is explicit in the order parameter and the nonlinearity is rather modest, the numerical integration poses no particular problems and can be accomplished with either standard methods, or the so-called cell-dynamical systems method.^{15–17}

Despite the elegance of the phenomenological approach and the simplicity of the resulting equations, it also has an obvious drawback. The method is ill-suited for dealing with the enormous variety of different molecular interactions which are typically found in complex fluids. There is little practicality in fitting phenomenological parameters to each different system. In addition the limited expansion may not include the pertinent symmetries of the system under investigation.

In view of the practical importance of working with more realistic molecular models, an extension of the theoretical and simulation methods to general nonlinear transport models and free energy functionals is clearly needed.

B. Application of free energy expansions

In our group we are investigating the practical application of the Langevin equations to the phase separation of polymer and surfactant mixtures, using a free energy functional derived for a collection of Gaussian chains in a mean-field environment. In this approach we try to retain as much as possible of the underlying molecular properties, i.e., the architecture and composition of the chains are important parameters. In previous papers we have studied the random term,⁶ the numerical calculation of the Gaussian chain density functional¹⁸ and we have presented some results of actual numerical calculations of phase separation in block copolymer melts,¹⁹ using a local exchange form for the transport coefficients. The latter paper also contains a full density functional derivation of the free energy functional and the Gaussian chain density functional for inhomogeneous off-equilibrium copolymer melts. In addition, a study of appropriate nonlocal transport coefficients is in progress.

During a simulation, the external potential, which can be derived from the free energy, has to be calculated repeatedly from the density. This was previously done using an iterative (time-consuming) inversion method. Here, we study the possibility of using more sophisticated explicit fourth-order free energy expansions for speeding up the calculations. The fourth-order expansion is derived from a functional Taylor expansion of the free energy functional, which differs in some subtle but important aspects from the older random phase approximation (RPA) of Leibler.²⁰ In our approach, the simple scalar coefficients of the phenomenological free energy models that were introduced in Sec. I A, are replaced by compound spatial operators, the so-called second-, third-, and fourth-order vertex coefficients.

There are three prerequisites for the practical applicability of fourth-order expansion methods as accurate explicit inversion algorithms. First, the expansion must be such that the second- and fourth-order vertices are both positive in the

entire frequency domain, in order to ensure that the fourth-order free energy expansion is sufficient to describe phase separation. Second, the expansion must account reasonably well for molecular details of the chain molecules, in particular chain architecture and composition. Third, the expansion must indeed lead to (much) faster numerical inversion algorithms.

We conclude that the fourth-order expansion scheme as defined in this paper, is not yet suited for our purpose, even if we retain all spatial properties of the second-, third-, and fourth-order vertex coefficients. The main reason is that in the block copolymer melt, it turns out that the fourth-order vertex is negative for certain wave vectors and hence, a fourth-order free energy expansion is not necessarily sufficient to describe phase separation in these cases.

However, we also show that the fourth-order vertex coefficient is positive for most wave vectors, implying that a fourth-order free energy expansion is sufficient for studying the relative stability of most ordered phases in order to derive a mean-field phase diagram,^{20–23} depending on which lattice wave vectors are taken into account. Using the present expansion for dynamics simulations however, requires at least a sixth-order expansion in some cases. The second reason why expansion methods are not well suited for the dynamic simulations is purely on the computational side. The fourth-order expansion is cast in the form of linear, bilinear, and trilinear operators, which are convolutions in direct space in respectively 3, 6, and 9 dimensions. These high-dimensional convolutions are extremely expensive computationally and cannot be used as such in numerical simulations. For the second- and third-order vertex coefficient we have succeeded in implementing a simple and accurate fitting procedure, which reduces the convolution kernels to a generalized rotationally symmetric gradient expansion in direct space. For the fourth-order vertex coefficients our proposed fitting scheme is no longer practical. However, our fitting scheme leads to a whole new class of phase-separation models, with nonphenomenological parameters that are based on microscopic information.

C. Outline of the paper

In Sec. II we briefly recapitulate the background of the free energy functional and the Gaussian chain density functional, in the framework of a highly simplified Langevin model. For sake of argument we limit most of the discussions to the case of a (block) copolymer melt. The extension of the arguments to more general multicomponent mixtures is trivial. In Sec. III we present the fourth-order expansions, and we make some comparison to and show the differences with RPA free energy expansions in Sec. III A. In Sec. IV we discuss new properties of the vertex coefficients. In Sec. V we discuss the fitting procedure, and the transformation to direct space gradient expansions.

II. THEORY

Suppose we have a copolymer melt of volume V , containing n diblock copolymer chains, each of length

$N = N_A + N_B$. We assume that the kinetic coefficients are constant ($\Lambda_{AA} = \Lambda_{BB} = \lambda$), we neglect any cross kinetic terms ($\Lambda_{AB} = \Lambda_{BA} = 0$) and set the noise to zero. In this highly simplified scheme the Langevin Eq. (1) reduce to a set of two coupled diffusion equations

$$\frac{\partial \rho_A}{\partial t} = \lambda \nabla^2 \mu_A, \quad (4)$$

$$\frac{\partial \rho_B}{\partial t} = \lambda \nabla^2 \mu_B. \quad (5)$$

These equations look very simple, but are highly nonlinear and strongly coupled through the Gaussian chain density functional. The density functional gives a closing set of relations between the chemical potentials and the density fields. The relation can easily be derived from the intrinsic free energy functional of the system, which is (for details see Ref. 19):

$$F[\rho_A, \rho_B] = -\beta^{-1} n \ln \Phi + \beta^{-1} \ln n! - \sum_I \int_V U_I(\mathbf{r}) \rho_I(\mathbf{r}) d\mathbf{r} + F^{\text{nid}}, \quad (6)$$

Φ is the partition functional, the sum \sum_I is over component types I (A or B) and $U_A(\mathbf{r})$ and $U_B(\mathbf{r})$ are external potentials, conjugate to the particle density fields $\rho_A(\mathbf{r})$ and $\rho_B(\mathbf{r})$. The nonideal free energy functional F^{nid} contains the mean-field (excluded volume and cohesive) interactions between the chains. Since in this paper we are only concerned with the relation between the external potential and the density fields, and the mean field contains by definition only the density fields, the precise form of the nonideal interactions is inconsequential. Notice however that in comparing our results to Leibler's RPA free energy expression,²⁰ we must remember that the RPA results are derived including the mean field, which adds a Flory–Huggins interaction term to the second-order vertex coefficient of the free energy expansion. It is important to realize that we do not assume incompressibility at this stage; the expansion is derived for a compressible melt.

The Gaussian chain density functional is defined by

$$\rho_I[U_A, U_B](\mathbf{r}) = n \text{Tr}_c \psi \hat{\rho}_I, \quad (7)$$

where $\hat{\rho}_I(\mathbf{r})$ is a single chain microscopic density operator, defined by

$$\hat{\rho}_I(\mathbf{r}) \equiv \sum_{s=1}^N \delta_{I_s}^K \delta(\mathbf{r} - \mathbf{R}_s), \quad (8)$$

$\delta_{I_s}^K$ is a Kronecker delta function, with value 1 if bead s is of type I (A or B) and 0 otherwise, \mathbf{R}_s is the coordinate of bead s . The single chain trace Tr_c is the integration over the coordinate space of one chain only

$$\text{Tr}_c(\cdot) \equiv \frac{1}{\mathcal{N}} \int_{V^N} (\cdot) \prod_{s=1}^N d\mathbf{R}_s, \quad (9)$$

where \mathcal{N} is a normalization constant with dimension $(\text{Length})^{3N}$. The single chain distribution function ψ and the partition functional Φ are defined by

$$\psi \equiv \frac{1}{\Phi} \exp \left\{ -\beta \left[H^G + \sum_{s=1}^N U_s(\mathbf{R}_s) \right] \right\}, \quad (10)$$

$$\Phi \equiv \text{Tr}_c \exp \left\{ -\beta \left[H^G + \sum_{s=1}^N U_s(\mathbf{R}_s) \right] \right\}. \quad (11)$$

H^G is the standard Edwards Hamiltonian for the Gaussian chain^{24,25}

$$H^G = \frac{\beta^{-1} 3}{2a^2} \sum_{s=2}^N (\mathbf{R}_s - \mathbf{R}_{s-1})^2, \quad (12)$$

where a is the Gaussian bond length parameter. Finally, the intrinsic chemical potentials μ_I are related to the external potentials via

$$\mu_I = \frac{\delta F}{\delta \rho_I} = \frac{\delta F^{\text{nid}}}{\delta \rho_I} - U_I. \quad (13)$$

The density functional (7) is a *bijective* relation between the external potentials and the conjugate density fields.²⁶ In our previous work we inverted the density functional numerically by an iteration technique,¹⁹ which is very time consuming. Here, the problem is to find an explicit expression for the external potentials in terms of the density fields, by an analytical Taylor expansion method, which can be used in the dynamics algorithm.

III. EXPANSION METHOD

We consider deviations from the homogeneous state, for which $\rho_I(\mathbf{r}) = \rho_I^0$, and $U_I = 0$. The fourth order Taylor expansion of the free energy in powers of the external potential is (cf. Ref. 20)

$$F = F^{\text{nid}} + F_0^{\text{id}} + \sum_{k=1}^4 \frac{(-\beta)^{k-1}}{k!} \sum_{\{I\}_k} \int_{V^k} G_{\{I\}_k}^{(k)}(\mathbf{r}, \dots, \mathbf{r}_{k-1}) \times U_{I_0}(\mathbf{r}) \cdots U_{I_{k-1}}(\mathbf{r}_{k-1}) d\mathbf{r} \cdots d\mathbf{r}_{k-1}. \quad (14)$$

The summations $\sum_{\{I\}_k}$ are over all component types, i.e., $\{I\}_1 = I$, $\{I\}_2 = IJ$, $\{I\}_3 = IJK$, and $\{I\}_4 = IJKL$, and $I_k = I, J, K$, or L . The superscripts indicate the order of the kernels. The Taylor coefficients of the expansion are n -body correlators which reduce to n -particle densities in the limit $n \rightarrow \infty$

$$G_I^{(1)}(\mathbf{r}) = n \langle \hat{\rho}_I \rangle_0 = \rho_I^0, \quad (15)$$

$$G_{IJ}^{(2)}(\mathbf{r}, \mathbf{r}_1) = n \langle \hat{\rho}_I(\mathbf{r}) \hat{\rho}_J(\mathbf{r}_1) \rangle_0, \quad (16)$$

$$G_{IJK}^{(3)}(\mathbf{r}, \mathbf{r}_1, \mathbf{r}_2) = n \langle \hat{\rho}_I(\mathbf{r}) \hat{\rho}_J(\mathbf{r}_1) \hat{\rho}_K(\mathbf{r}_2) \rangle_0, \quad (17)$$

$$G_{IJKL}^{(4)}(\mathbf{r}, \mathbf{r}_1, \mathbf{r}_2, \mathbf{r}_3) = n \langle \hat{\rho}_I(\mathbf{r}) \hat{\rho}_J(\mathbf{r}_1) \hat{\rho}_K(\mathbf{r}_2) \hat{\rho}_L(\mathbf{r}_3) \rangle_0. \quad (18)$$

The averages $\langle \cdot \rangle_0 \equiv [\Phi^{-1} \text{Tr}_c(\cdot)]_{U=0}$ are single chain ensemble averages, using the distribution function of the Gaussian chain in the homogeneous melt. Since the homogeneous melt is translationally invariant, we can set

$$G_{IJ}^{(2)}(\mathbf{r}, \mathbf{r}_1) = G_{IJ}^{(2)}(\mathbf{r} - \mathbf{r}_1), \quad (19)$$

$$G_{IJK}^{(3)}(\mathbf{r}, \mathbf{r}_1, \mathbf{r}_2) = G_{IJK}^{(3)}(\mathbf{r} - \mathbf{r}_1, \mathbf{r} - \mathbf{r}_2), \quad (20)$$

$$G_{IJKL}^{(4)}(\mathbf{r}, \mathbf{r}_1, \mathbf{r}_2, \mathbf{r}_3) = G_{IJKL}^{(4)}(\mathbf{r} - \mathbf{r}_1, \mathbf{r} - \mathbf{r}_2, \mathbf{r} - \mathbf{r}_3). \quad (21)$$

Employing the translational invariance at this stage simplifies the derivation of the inverse density expansion compared to RPA considerably, as can be seen from Eqs. (26)–(28). The expansion of the density functional reads

$$\begin{aligned} \tilde{\rho}_I(\mathbf{r}) = & \sum_{k=1}^3 \frac{(-\beta)^k}{k!} \sum_{\{I\}_k} \int_{V^k} G_{\{I\}_{k+1}}^{(k+1)}(\mathbf{r} - \mathbf{r}_1, \dots, \mathbf{r} - \mathbf{r}_k) \\ & \times U_{I_1}(\mathbf{r}_1) \cdots U_{I_k}(\mathbf{r}_k) d\mathbf{r}_1 \cdots d\mathbf{r}_k, \end{aligned} \quad (22)$$

where $\tilde{\rho}_I(\mathbf{r})$ is the deviation from homogeneous density

$$\tilde{\rho}_I(\mathbf{r}) \equiv \rho_I(\mathbf{r}) - \rho_I^0. \quad (23)$$

Notice that we have as many order parameters as there are component types, which are retained throughout the calculations. The inverse expansion for the external potential is given by

$$\begin{aligned} U_I(\mathbf{r}) = & -k_B T \sum_{k=1}^3 \frac{1}{k!} \sum_{\{I\}_k} \int_{V^k} \Gamma_{\{I\}_{k+1}}^{(k+1)}(\mathbf{r} - \mathbf{r}_1, \dots, \mathbf{r} - \mathbf{r}_k) \\ & \times \tilde{\rho}_{I_1}(\mathbf{r}_1) \cdots \tilde{\rho}_{I_k}(\mathbf{r}_k) d\mathbf{r}_1 \cdots d\mathbf{r}_k, \end{aligned} \quad (24)$$

which introduces the second-, third-, and fourth-order vertex coefficients $\Gamma_{IJ}^{(2)}$, $\Gamma_{IJK}^{(3)}$, and $\Gamma_{IJKL}^{(4)}$, respectively. By integration of the chemical potentials (13) we obtain the free energy expansion in the density fields

$$\begin{aligned} F = & F^{\text{nid}} + F_0^{\text{id}} + k_B T \sum_{k=2}^4 \frac{1}{k!} \sum_{\{I\}_k} \int_{V^k} \Gamma_{\{I\}_k}^{(k)}(\mathbf{r} - \mathbf{r}_1, \dots, \mathbf{r} - \mathbf{r}_{k-1}) \\ & \times \tilde{\rho}_{I_0}(\mathbf{r}) \cdots \tilde{\rho}_{I_{k-1}}(\mathbf{r}_{k-1}) d\mathbf{r} \cdots d\mathbf{r}_{k-1}, \end{aligned} \quad (25)$$

where we have set the average of the external potentials to zero [$\int_V U_I(\mathbf{r}) d\mathbf{r} = 0$].

The vertex coefficients and the n -body correlators are convolution kernels in 3, 6, and 9 dimensions, hence the expansions have a simpler representation in Fourier space. We define the Fourier transform of a function f by $f(\mathbf{q}) = \int_V e^{i\mathbf{q}\cdot\mathbf{r}} f(\mathbf{r}) d\mathbf{r}$ and the inverse transform by

$$f(\mathbf{r}) = \frac{1}{(2\pi)^3} \int_V e^{-i\mathbf{q}\cdot\mathbf{r}} f(\mathbf{q}) d\mathbf{q}.$$

We then apply a one-step iteration technique (substituting the expansions for U_I in the expansions for $\tilde{\rho}_I$) to obtain analytical relations between the vertex coefficients and the n -body correlators in Fourier space. For simplification, we can use a matrix notation (indicated with subscript M) which may be compared to formulas (III-14)–(III-16) in Ref. 20, but is structurally different:

$$I_M = G_M^{(2)}(\mathbf{q}) \Gamma_M^{(2)}(\mathbf{q}), \quad (26)$$

$$\begin{aligned} 0_M = & G_M^{(2)}(\mathbf{q}_1 + \mathbf{q}_2) \Gamma_M^{(3)}(\mathbf{q}_1, \mathbf{q}_2) + G_M^{(3)}(\mathbf{q}_1, \mathbf{q}_2) \Gamma_M^{(2)}(\mathbf{q}_1) \\ & \otimes \Gamma_M^{(2)}(\mathbf{q}_2), \end{aligned} \quad (27)$$

$$\begin{aligned} 0_M = & G_M^{(2)}(\mathbf{q}_1 + \mathbf{q}_2 + \mathbf{q}_3) \Gamma_M^{(4)}(\mathbf{q}_1, \mathbf{q}_2, \mathbf{q}_3) \\ & + G_M^{(4)}(\mathbf{q}_1, \mathbf{q}_2, \mathbf{q}_3) \Gamma_M^{(2)}(\mathbf{q}_1) \otimes \Gamma_M^{(2)}(\mathbf{q}_2) \otimes \Gamma_M^{(2)}(\mathbf{q}_3) \\ & + \frac{3}{2} G_M^{(3)}(\mathbf{q}_1, \mathbf{q}_2 + \mathbf{q}_3) \Gamma_M^{(2)}(\mathbf{q}_1) \otimes \Gamma_M^{(3)}(\mathbf{q}_2, \mathbf{q}_3) \\ & + \frac{3}{2} G_M^{(3)}(\mathbf{q}_1 + \mathbf{q}_2, \mathbf{q}_3) \Gamma_M^{(3)}(\mathbf{q}_1, \mathbf{q}_2) \otimes \Gamma_M^{(2)}(\mathbf{q}_3). \end{aligned} \quad (28)$$

Here \otimes denotes a Kronecker or direct matrix product,²⁷ which is defined in the following way: If A is a $m \times n$ matrix and B is a $p \times q$ matrix, then $A \otimes B$ is an $mp \times nq$ matrix given by

$$A \otimes B = \begin{bmatrix} a_{11}B & \cdots & a_{1n}B \\ \vdots & \ddots & \vdots \\ a_{m1}B & \cdots & a_{mn}B \end{bmatrix},$$

0_M is the zero matrix, I_M is the identity matrix. The matrices contain all expansion kernels in a logical order component wise, e.g., the $\{I, J\}$ element of $G_M^{(2)}(\mathbf{q})$ is given by $G_{IJ}^{(2)}(\mathbf{q})$. The n -body correlators can be calculated in Fourier space according to the formulas given in Appendix A.

Notice that the expression for relating $\Gamma^{(4)}$ to the n -body correlators $G^{(2)}$, $G^{(3)}$, and $G^{(4)}$ is different from the usual RPA expression (Appendix B). The relation for $\Gamma^{(4)}$ as obtained from a straightforward application of the one-step iteration technique, does not necessarily possess all physical symmetries (such as rotational symmetry in its wave vectors). The relation can easily be symmetrized for a one-order parameter system as is done in Ref. 20, but symmetrization of the relations for a multicomponent compressible system leads to very complex expressions (see Appendix B for explanation). However, our nonsymmetric relations lead to an expansion for the external potential of the same accuracy and can hence be used to study the applicability of fourth-order expansions to the mesoscopic dynamics algorithms. In that case, the physical symmetries of $\Gamma^{(4)}$ are in principle not significant, as opposed to the symmetries of Γ_4 in the study of the stability of ordered phases.

A. Comparison with RPA

We want to stress that the above analysis contains some important differences with Leibler's RPA results.²⁰ From the onset, we assume that the system is a compressible collection of Gaussian chains in a mean-field environment, whereas in Leibler's RPA the system is incompressible, and the Gaussian chain approximation is made only after the expansion. This implies that here we have retained two relations between two density fields and two external potentials, rather than a single relation between one order parameter and one effective external potential as in the Leibler RPA. However, the underlying molecular model of ideal Gaussian chains in a mean field is the same. In fact, from a technical point of view we find that the route to the incompressible systems *via* the compressible expansion of Gaussian chain statistical behavior is much easier to handle than solving the RPA set directly, mainly because we make use of the translational in-

variance of the melt *before* Fourier transformation. This procedure also leads to different expressions for the free energy expansion and its vertex coefficients.

For a two-component incompressible system, the separate vertex coefficients can easily be connected to the vertex coefficients for a one-order-parameter system. In the incompressible system we define $\phi(\mathbf{r}) \equiv \tilde{\rho}_A(\mathbf{r})$ as the order parameter. By substituting $U(\mathbf{r}) \equiv U_A(\mathbf{r}) - U_B(\mathbf{r})$ and $\tilde{\rho}_B(\mathbf{r}) \equiv -\tilde{\rho}_A(\mathbf{r})$ we define

$$\Gamma^{(2)} \equiv \Gamma_{AA}^{(2)} - \Gamma_{AB}^{(2)} - \Gamma_{BA}^{(2)} - \Gamma_{BB}^{(2)}, \quad (29)$$

$$\Gamma^{(3)} \equiv \Gamma_{AAA}^{(3)} - \Gamma_{AAB}^{(3)} - \Gamma_{ABA}^{(3)} + \Gamma_{ABB}^{(3)} - \Gamma_{BAA}^{(3)} + \Gamma_{BAB}^{(3)} + \Gamma_{BBA}^{(3)} - \Gamma_{BBB}^{(3)}, \quad (30)$$

$$\Gamma^{(4)} \equiv \Gamma_{AAAA}^{(4)} - \Gamma_{AAAB}^{(4)} - \Gamma_{AABA}^{(4)} + \Gamma_{AABB}^{(4)} - \Gamma_{ABAA}^{(4)} + \Gamma_{ABAB}^{(4)} + \Gamma_{ABBA}^{(4)} - \Gamma_{ABBB}^{(4)} - \Gamma_{BAAA}^{(4)} + \Gamma_{BAAB}^{(4)} + \Gamma_{BABA}^{(4)} - \Gamma_{BABB}^{(4)} + \Gamma_{BBAA}^{(4)} - \Gamma_{BBAB}^{(4)} - \Gamma_{BBBB}^{(4)} + \Gamma_{BBBB}^{(4)}. \quad (31)$$

Our combined vertex coefficients $\Gamma^{(2)}$ and $\Gamma^{(3)}$ may now be linked to the Leibler coefficients of the free energy expansion Γ_2 and Γ_3 in Ref. 20 in the following manner:

$$\Gamma^{(2)}(\mathbf{q}) = \Gamma_2(\mathbf{q}, -\mathbf{q}) \quad (\chi=0), \quad (32)$$

$$\Gamma^{(3)}(\mathbf{q}_1, \mathbf{q}_2) = \Gamma_3(\mathbf{q}_1 + \mathbf{q}_2, -\mathbf{q}_1, -\mathbf{q}_2). \quad (33)$$

These relations follow from a direct comparison of Eqs. III-22 and III-23 in Ref. 20 to Eqs. (26) and (27) keeping both free energy expressions in mind. Notice that the relations for $\Gamma^{(2)}$ and $\Gamma^{(3)}$ are unique and automatically possess all physical symmetries. We explain how $\Gamma^{(4)}$ can be symmetrized in Appendix B.

IV. PROPERTIES OF VERTEX COEFFICIENTS

For a diblock copolymer compact Debye type formulas can be derived for $G_{IJ}^{(2)}$, $G_{IJK}^{(3)}$, and $G_{IJKL}^{(4)}$, in terms of N , N_A , and N_B by simply writing out all summations (see Appendix A). We have calculated the n -body correlators both for arbitrary chain length and all \mathbf{q} and also for the limit of very long chains and small \mathbf{q} (that is, when $N \rightarrow \infty$, $a^2 \mathbf{q}^2/6 \rightarrow 0$ and $Na^2 \mathbf{q}^2/6$ remains finite, which is the limit considered by the RPA). The vertex coefficients are obtained by inserting the formulas for the n -body correlators in the inversion relations. The formulas can in our approach readily be calculated by computational algebra methods because they do not involve summations over wave vectors. However, especially the formulas for the higher order vertex coefficients are unwieldy, and therefore, they will not be included here. A *Mathematica* script for generating the analytical formulas for the n -body correlators and the vertex coefficients is available on request from the authors. As far as we know, the *full* wave vector dependence has not been

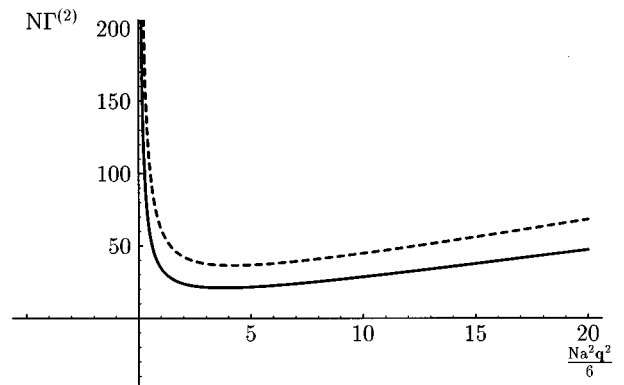


FIG. 1. $N\Gamma^{(2)}$ in the limit of very long chains as a function of $Na^2\mathbf{q}^2/6$ for different compositions. —: $f=1/2$, - -: $f=1/4$.

calculated before for $\Gamma^{(3)}$ and $\Gamma^{(4)}$. We will now briefly discuss each of the combined vertex coefficients for the incompressible system, which is especially important for understanding how an accurate and calculatable explicit inverse density expansion must be derived that includes all wave-vector dependencies. Discussing the separate vertex coefficients is also possible, but is cumbersome and does not allow comparison with low order RPA free energy expansions.

A. $\Gamma^{(2)}$

This coefficient is well known and can be related to Γ_2 in Ref. 20. See Fig. 1 for a few examples. $\Gamma^{(2)}$ [see Eqs. (26) and (29)] is singular and scales with \mathbf{q}^{-2} , hence density fluctuations on scales larger than the polymer coil size are unfavorable. Here we notice an additional property on monomer length scales which is not usually discussed, but is nevertheless important for numerical applications. We have

$$\lim_{|\mathbf{q}| \rightarrow \infty} \Gamma^{(2)}(\mathbf{q}) = \frac{N^2}{N_A N_B}. \quad (34)$$

Hence this limit is finite for any chain length. Physically, the limiting value indicates that if the external potential has a period that gradually decreases to monomer length scales, the response of the chain does not further change. As we will see in Sec. V A, the behavior of $\Gamma^{(2)}$ in general and especially the influence of the limiting value for large $|\mathbf{q}|$ cannot be neglected in a gradient free energy expansion for systems with widespread density spectra.

B. $\Gamma^{(3)}$

Assume first, without loss of generality, that $\mathbf{q}_1 = \mathbf{q}_2 = \mathbf{q}$. We approximate

$$e^{-(a^2 \mathbf{q}^2)/6} \approx 1 - \frac{a^2 \mathbf{q}^2}{6} + \frac{a^4 \mathbf{q}^4}{36} - \frac{a^6 \mathbf{q}^6}{216}. \quad (35)$$

Employing the inversion relations (27) and (30) this yields

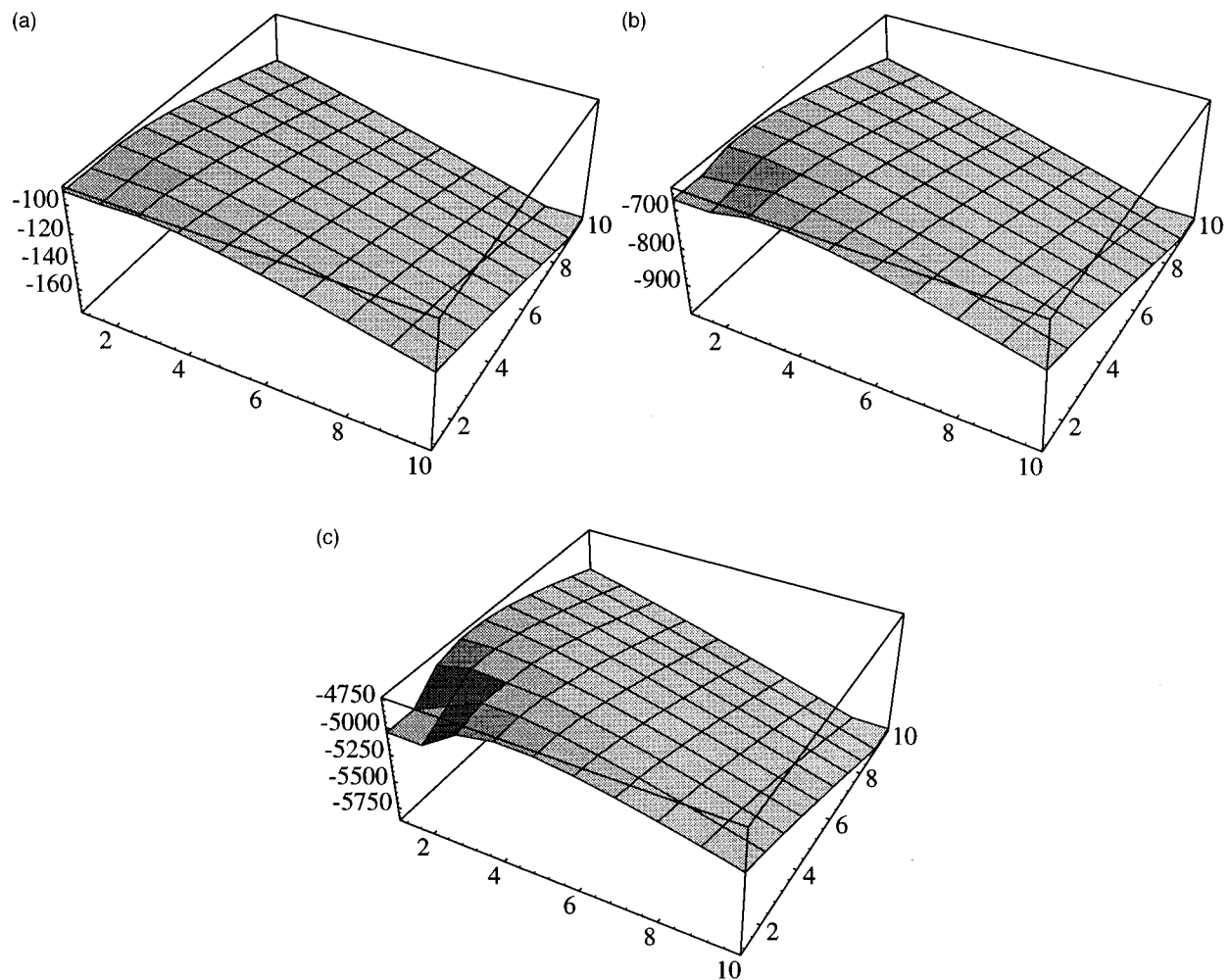


FIG. 2. $N\Gamma^{(3)}$ in the limit of very long chains as a function of $(Na^2\mathbf{q}_1^2)/6$ and $(Na^2\mathbf{q}_2^2)/6$, $\mathbf{q}_1 \cdot \mathbf{q}_2 = 0$. (a) $f = 1/4$, (b) $f = 1/8$, (c) $f = 1/16$.

$$\lim_{|\mathbf{q}| \rightarrow 0} \Gamma^{(3)}(\mathbf{q}, \mathbf{q}) = - \frac{N(N_B^2 - N_A^2)[6 + 30N^2 + N_A N_B(3 + 23N^2 - 5N_A N_B)]}{4N_A N_B(1 + 2N_A N_B)^3}. \quad (36)$$

Hence, we find that $\Gamma^{(3)}$ is *not* singular near the origin, in contrast to $\Gamma^{(2)}$. We may investigate the limit in infinity for $\mathbf{q}_1 = \mathbf{q}_2 = \mathbf{q}$ and check that the result agrees with well-known results from, e.g., Ref. 21. We find that

$$\lim_{|\mathbf{q}| \rightarrow \infty} \Gamma^{(3)}(\mathbf{q}, \mathbf{q}) = - \frac{N^3}{N_A^2 N_B^2} (N_B - N_A). \quad (37)$$

Also notice that this limit does not depend on chain length, but only on the ratio $f \equiv N_A/N_B$. In the limit of very long chains, $\Gamma^{(3)}$ strongly depends on f as can be seen in Fig. 2, where $\Gamma^{(3)}$ is plotted for four different values of f . We see that the optimum becomes more distinct if the asymmetry of the chain increases. Notice that the full wave vector dependence of $\Gamma^{(3)}$ is depicted.

C. $\Gamma^{(4)}$

First, we again emphasize that $\Gamma^{(4)}$ is only comparable to the RPA fourth-order vertex function Γ_4 after the extra symmetrization step (Appendix B). Here we study the bare unsymmetric $\Gamma^{(4)}$ coefficient which was derived directly from the one-step iteration method. In calculating $\Gamma^{(4)}$ in the limit of very long chains and small \mathbf{q} (see Fig. 3, \mathbf{q}_1 , \mathbf{q}_2 , and \mathbf{q}_3 are parallel) we find that if \mathbf{q}_1 and \mathbf{q}_2 or \mathbf{q}_2 and \mathbf{q}_3 are small, $\Gamma^{(4)}$ is negative and if \mathbf{q}_1 and \mathbf{q}_3 are small, $\Gamma^{(4)}$ is positive. Near the origin, $\Gamma^{(4)}$ is positive and singular. From these results we conclude that $\Gamma^{(4)}$ is not necessarily positive in the entire Fourier domain. In calculating $\Gamma^{(4)}$ for other orientations of the three frequencies, we find that $\Gamma^{(4)}$ changes sign in many more cases. From Fig. 3 we conclude that the area where $\Gamma^{(4)}$ is negative becomes larger if the chain becomes more symmetric (in the limit of very long

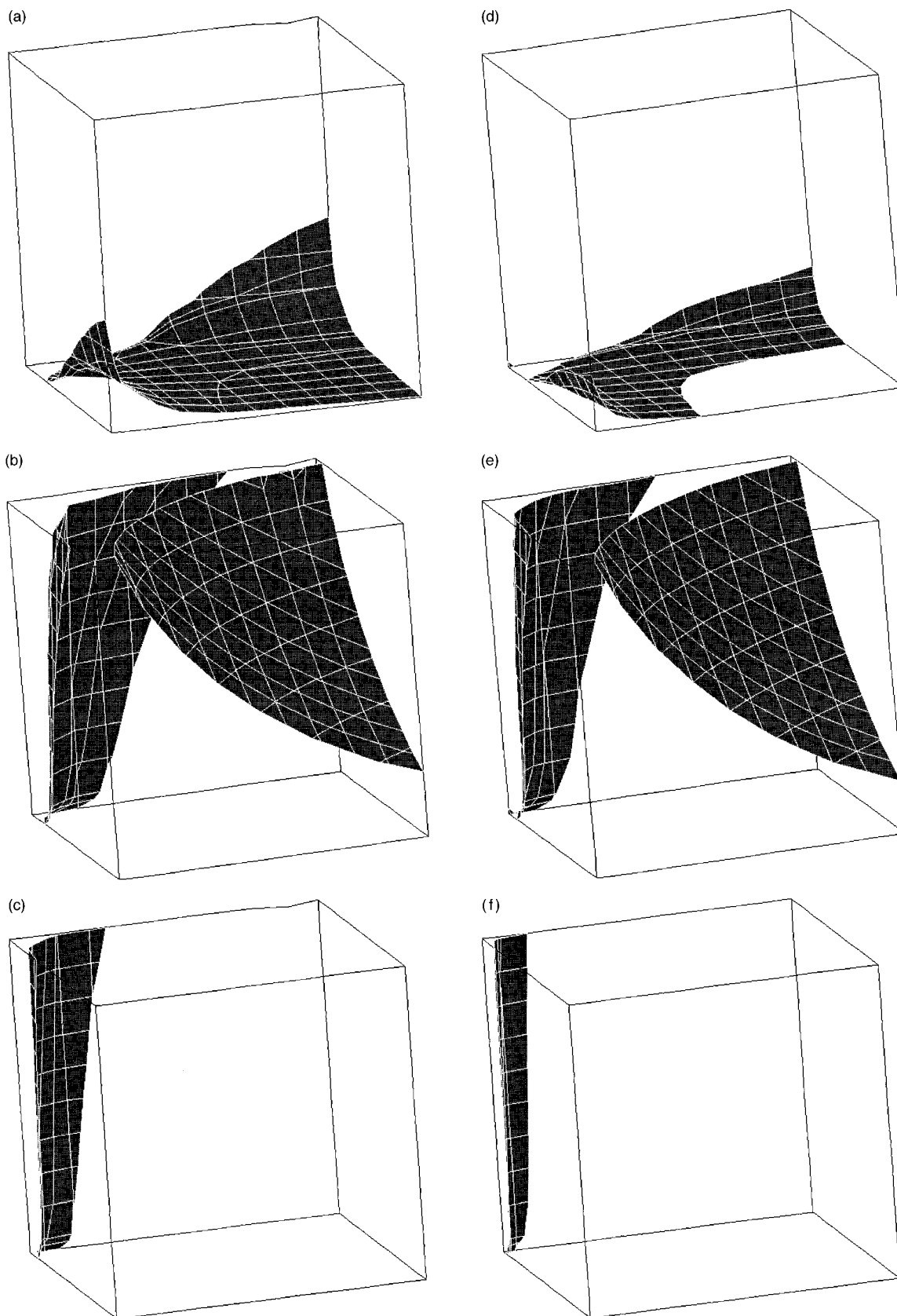


FIG. 3. Isosurfaces of $N\Gamma^{(4)}$ in the limit of very long chains as a function of $(Na^2\mathbf{q}_1^2)/6$, $(Na^2\mathbf{q}_2^2)/6$, and $(Na^2\mathbf{q}_3^2)/6$. \mathbf{q}_1 , \mathbf{q}_2 , and \mathbf{q}_3 are parallel, $0.1 \leq (Na^2\mathbf{q}_i^2)/6 \leq 9.5$ (small irregularities are due to the isosurface calculation which is based on 1000 data points) (a) $f=1/2$, isosurface $N\Gamma^{(4)}=0$, (b) $f=1/2$, isosurface $N\Gamma^{(4)}=550$, (c) $f=1/2$, isosurface $N\Gamma^{(4)}=1000$, (d) $f=1/4$, isosurface $N\Gamma^{(4)}=0$, (e) $f=1/4$, isosurface $N\Gamma^{(4)}=2500$, (f) $f=1/4$, isosurface $N\Gamma^{(4)}=5000$.

chains). The behavior of $\Gamma^{(4)}$ seems to be singular for \mathbf{q}_1 and \mathbf{q}_3 small, but along the other axes the function seems to decrease only linearly.

We realize however that these results may be influenced by the particular choice for $\Gamma^{(4)}$, i.e., which particular symmetry is chosen. We have not performed the calculations of the symmetrized $\Gamma^{(4)}$ because of the complexity, but intend to do so for a multicomponent compressible system in the near future.

D. Remarks

In a Ginzburg–Landau fourth-order model for the free energy the second-order term must have a negative sign and the fourth-order term must have a positive sign in order to obtain the two minima that are necessary to describe a phase-separated system.²⁸ If we translate this concept to the case of the copolymer melts, the second- and fourth-order terms in the inverse density expansion must preferably have the same sign; the second-order term changes sign if the melt is quenched (which effectively instantaneously increases the interaction parameter χ), which shifts part of $\Gamma^{(2)}(\mathbf{q})$ to negative values.

Since the expansion we consider here is more complex than a simple polynomial (because the full wave vector dependence is considered and the expansion terms consist of high-dimensional integrals), we must carefully examine the consequences of the above remarks in the different limits. In the weak segregation limit, the density may be approximated by a single Fourier component for an ordered structure. This Fourier component is determined by the optimum \mathbf{q}^* of $\Gamma^{(2)}$. In order to describe phase-separation,

$$\begin{aligned} & \int_{V^4} \Gamma^{(4)}(\mathbf{r}-\mathbf{r}_1, \mathbf{r}-\mathbf{r}_2, \mathbf{r}-\mathbf{r}_2) \phi(\mathbf{r}) \phi(\mathbf{r}_1) \phi(\mathbf{r}_2) \phi(\mathbf{r}_3) \\ & \times d\mathbf{r} d\mathbf{r}_1 d\mathbf{r}_2 d\mathbf{r}_3 \\ & = \frac{1}{(2\pi)^9} \int_{V^3} \Gamma^{(4)}(\mathbf{q}_1, \mathbf{q}_2, \mathbf{q}_3) \phi(-\mathbf{q}_1 - \mathbf{q}_2 - \mathbf{q}_3) \\ & \times \phi(\mathbf{q}_1) \phi(\mathbf{q}_2) \phi(\mathbf{q}_3) d\mathbf{q}_1 d\mathbf{q}_2 d\mathbf{q}_3, \end{aligned} \quad (38)$$

must be positive [remember that in the incompressible system the order parameter $\phi(\mathbf{r}) = \tilde{\rho}_A(\mathbf{r})$]. Since the sign of the coefficient $\Gamma^{(4)}$ changes depending on \mathbf{q}^* , the sign of the integral (38) will depend on the density spectrum. In the weak segregation limit $|\mathbf{q}_1| = |\mathbf{q}_2| = |\mathbf{q}_3|$ and $|\mathbf{q} - \mathbf{q}_1 - \mathbf{q}_2| = |\mathbf{q}^*|$, but the angles between these vectors are still free and are determined by the ordered mesophase under consideration.

In the strong segregation limit and for nonordered structures, the density spectrum is much more wide spread. In this case it is a very bad approximation to represent the density by a single harmonic or even by multiple harmonics. Many authors have mentioned this before in the context of the study of the relative stability of ordered structures (e.g., Refs. 22, 23, 29, and 30). Also in self consistent field approximations it is noted that an increasing number of basis functions is needed in the strong segregation limit (e.g., Refs. 31–33).

The widespread density spectrum in numerical simulations of ordering processes in metastable irregular structures, implies that there may exist a negative contribution from Eq. (38) now, caused by the Fourier components of the density in the part of the spectrum where $\Gamma^{(4)}$ is negative. Depending on the balance between positive and negative contributions, a fourth-order functional Taylor expansion may no longer be sufficient to describe the phase-separated system in a simulation. In these cases, a sixth-order functional Taylor expansion may have to be made to obtain an explicit expression for the inverse density (external potential) expansion. The fourth-order external potential expansion may however serve as a preconditioner in the previously used iterative inversion schemes (see Refs. 19 and 34). As mentioned before, we intend to study the sign of the symmetrized $\Gamma^{(4)}$ in the near future.

V. FITTING PROCEDURE

Now we return to the simplified Langevin models (4) and (5). We recall that our main goal is to calculate the $\nabla^2 \mu_I$ terms as efficiently as possible for numerical simulations of microphase separation, given the analytical Fourier transforms of the vertex coefficients. We do not restrict the system to incompressibility, and hence we must examine each of the individual coefficients $\Gamma_{IJ}^{(2)}$, $\Gamma_{IJK}^{(3)}$, $\Gamma_{IJKL}^{(4)}$, separately. Since the expansion of the external potential (24) consists of linear, bilinear, and trilinear terms, which are multi-dimensional convolutions, one expects the numerical calculations to become easier in Fourier space. This is partly true. The linear term is simply a multiplication in Fourier space, but the bilinear term still involves a complicated integration in three dimensions. This is not well suited for numerical integration. This applies even more so to the trilinear terms which are six dimensional integrations in Fourier space. In this form the external potential expansion is not yet suited for application in the dynamics algorithms.

The main principle of the method we propose here is that the vertex coefficients are fitted by well-chosen polynomial series of wave vectors. The polynomial series can easily be inverse Fourier transformed, which results in relatively compact gradient expansions. These gradient expansions can then be discretized by traditional methods and calculated numerically, which allows application of the external potential expansion in the mesoscopic dynamics algorithms. The linear, bilinear, and trilinear terms will now be discussed in detail.

A. Linear term

The complexity of the linear terms consists of two parts; all $\Gamma_{IJ}^{(2)}$ scale with \mathbf{q}^{-2} near the origin, and all $\Gamma_{IJ}^{(2)}$ have a plateau region for large \mathbf{q} [see Eq. (34)]. These properties make it hard to calculate an accurate and compact discrete representation in the *entire* \mathbf{q} domain. We remove the singularity by considering the expansion for $\nabla^2 U_I$ instead of U_I , i.e., in Fourier space we expand $-\mathbf{q}^2 U_I(\mathbf{q}) = -\mathbf{q}^2 \sum_J \Gamma_{IJ}^{(2)}(\mathbf{q}) \tilde{\rho}_J(\mathbf{q}) + \dots$. We have found that $\mathbf{q}^2 \Gamma_{IJ}^{(2)}(\mathbf{q})$ can be approximated by a series expansion of the

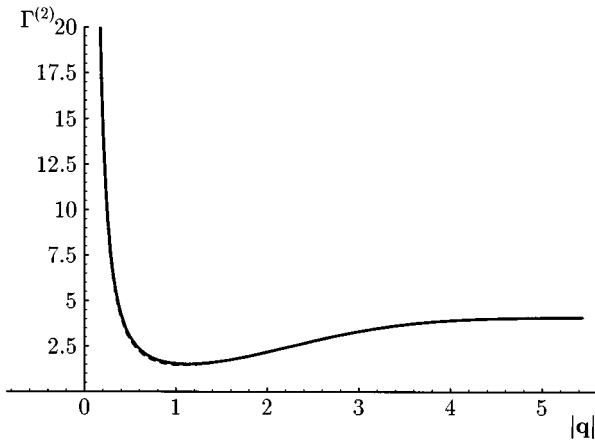


FIG. 4. Analytical (—) and fitted (---) $\Gamma^{(2)}$ for A_3B_6 as a function of $|\mathbf{q}|$.

form $\sum_{i=0}^l c_{iIJ} \mathbf{q}^{2i}$. For $\Gamma_{IJ}^{(2)}$ we employ a least-squares fitting procedure, using 10 datapoints (taking into account spherical symmetry) and a varying number of fit functions. If the length of the chain increases, the optimum of $\Gamma^{(2)}$ shifts towards lower frequencies, the optimum becomes more distinct and the plateau, that was discussed in Sec. IV A, becomes a larger part of the fit domain. Because the plateau is hard to fit with a limited number of fit functions, the number of fit functions increases with increasing chain length. In Fig. 4 we check the accuracy by comparing the analytical and fitted combined vertex coefficient $\Gamma^{(2)}$ for the chain A_3B_6 for the incompressible athermal melt. We see that the accuracy is perfect, albeit at the cost of a rather large number of fit functions (eight in this case). We can now inverse Fourier transform the linear term in the inverse expansion and find the approximation in direct space

$$\begin{aligned} \nabla^2 \sum_J \int_V \Gamma_{IJ}^{(2)}(\mathbf{r}-\mathbf{r}_1) \tilde{\rho}_J(\mathbf{r}_1) d\mathbf{r}_1 \\ \approx \sum_J c_0 - \nabla^2 [c_1 - \nabla^2 (c_2 - \dots)] \tilde{\rho}_J. \end{aligned} \quad (39)$$

The coefficients c_i are different for each combination IJ .

B. Bilinear term

We restrict ourselves to a demonstration of principle and discuss only the fitting of $\Gamma_{IJK}^{(3)}$ of a single chain architecture: A_3B_6 . Other architectures and longer chains can be treated using the same fitting procedure. Compared to $\Gamma_{IJ}^{(2)}$ the number of functions to be approximated now increases by a factor of 2 (from 4 to 8). Because of symmetry, only six functions have to be approximated effectively.

Although the combined $\Gamma^{(3)}$ shows rather simple nonsingular behavior, the independent $\Gamma_{IJK}^{(3)}$ show more complex and even singular behavior, which makes them harder to fit. Again we consider $\nabla^2 U_I$ which implies that we have to fit $(\mathbf{q}_1 + \mathbf{q}_2)^2 \Gamma_{IJK}^{(3)}(\mathbf{q}_1, \mathbf{q}_2)$. We find that the premultiplication removes the singularity in $(\mathbf{q}_1 + \mathbf{q}_2)^2 \Gamma_{AAA}^{(3)}(\mathbf{q}_1, \mathbf{q}_2)$ and $(\mathbf{q}_1 + \mathbf{q}_2)^2 \Gamma_{BBB}^{(3)}(\mathbf{q}_1, \mathbf{q}_2)$; but $(\mathbf{q}_1 + \mathbf{q}_2)^2 \Gamma_{AAB}^{(3)}$ and

$(\mathbf{q}_1 + \mathbf{q}_2)^2 \Gamma_{BBA}^{(3)}$ are still singular in one coordinate and $(\mathbf{q}_1 + \mathbf{q}_2)^2 \Gamma_{ABB}^{(3)}$ and $(\mathbf{q}_1 + \mathbf{q}_2)^2 \Gamma_{BAA}^{(3)}$ remain singular in both coordinates.

Compared to $\Gamma_{IJ}^{(2)}$ the number of data points for the least-squares fit per function now increases from 10 to 180. The set of data points is chosen such that it represents the characteristics of the behavior of each function sufficiently. The number of fit functions depends on the singularity in $\Gamma_{IJK}^{(3)}$. We find that the bilinear terms may be fitted using the fit functions indicated in Table I.

The accuracy of the fit results is considerable, some examples for $\Gamma_{AAA}^{(3)}$, $\Gamma_{AAB}^{(3)}$, and $\Gamma_{ABB}^{(3)}$ are given in Fig. 5. The results for the other $\Gamma_{IJK}^{(3)}$ are similar. The global behavior of the analytical and fitted results is the same and the range of the values agrees in all cases. In Fig. 6 we have plotted the analytical and fitted results for $(\mathbf{q}_1 + \mathbf{q}_2)^2 \Gamma^{(3)}(\mathbf{q}_1, \mathbf{q}_2)$ which show that even though the $\Gamma_{IJK}^{(3)}$ are fitted independently, the combinations $\Gamma^{(3)}$ agree very well.

We can now again inverse Fourier transform the bilinear terms in the approximation of the inverse density expansion. For $\Gamma_{AAA}^{(3)}$ and $\Gamma_{BBB}^{(3)}$ this yields an expansion of the following form:

$$\begin{aligned} \nabla^2 \int_V \Gamma_{IJK}^{(3)}(\mathbf{r}-\mathbf{r}_1, \mathbf{r}-\mathbf{r}_2) \tilde{\rho}_J(\mathbf{r}_1) \tilde{\rho}_K(\mathbf{r}_2) d\mathbf{r}_1 d\mathbf{r}_2 \\ \approx c_0 \tilde{\rho}_J \tilde{\rho}_K + c_1 \tilde{\rho}_K (\nabla^2 \tilde{\rho}_J) + c_2 \tilde{\rho}_K (\nabla^4 \tilde{\rho}_J) + c_3 \tilde{\rho}_J (\nabla^2 \tilde{\rho}_K) \\ + c_4 (\nabla^2 \tilde{\rho}_J) (\nabla^2 \tilde{\rho}_K) + c_5 \tilde{\rho}_J (\nabla^4 \tilde{\rho}_K) + c_6 \nabla^2 (\tilde{\rho}_J \tilde{\rho}_K) \\ + c_7 \nabla^2 (\tilde{\rho}_K (\nabla^2 \tilde{\rho}_J)) + c_8 \nabla^2 (\tilde{\rho}_J (\nabla^2 \tilde{\rho}_K)) \\ + c_9 \nabla^2 (\nabla^2 \tilde{\rho}_J \nabla^2 \tilde{\rho}_K) + c_{10} \nabla^4 (\tilde{\rho}_J \tilde{\rho}_K). \end{aligned} \quad (40)$$

As before, the polynomial coefficients c_i are different for each combination IJK . For other $\Gamma_{IJK}^{(3)}$ that have been fitted some extra nonlocal and gradient terms are added to the expansion, e.g., $\nabla(\nabla^2 \tilde{\rho}_J) \cdot \nabla(\nabla^2 \tilde{\rho}_K)$, $\nabla z_J \cdot \nabla \tilde{\rho}_K$ and $\nabla z_J \cdot \nabla(\nabla^2 \tilde{\rho}_K)$. Here

$$z_I(\mathbf{r}) \equiv \int_V \frac{\tilde{\rho}_I(\mathbf{r}_1)}{|\mathbf{r}-\mathbf{r}_1|} d\mathbf{r}_1. \quad (41)$$

The use of z_I implies that the singularity has not disappeared completely. Together this yields a rather complex rotationally symmetric gradient expansion. The coefficients c_i strongly depend on the architecture and composition of the chain. The expansion automatically includes the symmetries of the system under investigation.

C. Trilinear term

Initially we devoted a considerable effort into finding a systematic fitting scheme for the $\Gamma_{IJKL}^{(4)}$ functions, but unfortunately we failed to do so. The reason is simply that there are too many special cases to consider, and all of them need careful evaluation. The magnitude of the problem may be appreciated if it is realized that the number of independent vertex coefficients increases from eight in the bilinear term to 16 in the trilinear term in a binary system. Each coefficient now depends on three wave vectors. It is also very hard,

TABLE I. Coefficients times 10^4 in four digits accuracy for fitted $(\mathbf{q}_1 + \mathbf{q}_2)^2 \Gamma_{JK}^{(3)}$ for A_8B_6 .

Fit function	$\Gamma_{AAA}^{(3)}$	$\Gamma_{AAB}^{(3)}$	$\Gamma_{ABB}^{(3)}$	$\Gamma_{BAA}^{(3)}$	$\Gamma_{BBA}^{(3)}$	$\Gamma_{BBB}^{(3)}$
1	32720	-588.2	6177	4872	-961.3	55430
\mathbf{q}_1^2	-1071	-104.4	24.03	33.99	-127.5	-1811
\mathbf{q}_1^4	33.45	3.397	-4.438	-3.548	4.061	57.22
\mathbf{q}_2^2	-1365	64.89	8.611	18.77	47.87	-2305
$\mathbf{q}_1^2 \mathbf{q}_2^2$	-26.59	-2.409	-4.495	-5.963	-1.148	-46.35
\mathbf{q}_2^4	34.33	-0.7804	-3.139	-2.472	-0.09591	58.35
$(\mathbf{q}_1 + \mathbf{q}_2)^2$	-27570	260.0	-406.8	-283.5	309.1	-49237
$\mathbf{q}_1^2 (\mathbf{q}_1 + \mathbf{q}_2)^2$	-143.1	-6.717	7.686	4.398	-7.388	-244.1
$\mathbf{q}_2^2 (\mathbf{q}_1 + \mathbf{q}_2)^2$	-127.3	-7.791	6.968	3.963	-8.714	-217.1
$\mathbf{q}_1^2 \mathbf{q}_2^2 (\mathbf{q}_1 + \mathbf{q}_2)^2$	5.734	0.3438	-0.1505	-0.02024	0.3587	9.789
$(\mathbf{q}_1 + \mathbf{q}_2)^4$	0.4985	-1.670	2.825	2.154	-2.127	0.8540
$\mathbf{q}_1 \cdot \mathbf{q}_2$	0.0	149.7	-219.7	-168.1	194.4	0.0
$\mathbf{q}_1^2 (\mathbf{q}_1 \cdot \mathbf{q}_2)$	0.0	-3.852	8.309	6.954	-5.151	0.0
$\mathbf{q}_2^2 (\mathbf{q}_1 \cdot \mathbf{q}_2)$	0.0	-2.301	7.301	6.199	-3.735	0.0
$(\mathbf{q}_1 \cdot \mathbf{q}_2)^2$	0.0	6.286	-10.76	-8.129	7.937	0.0
$\mathbf{q}_1^2 \mathbf{q}_2^2 (\mathbf{q}_1 \cdot \mathbf{q}_2)$	0.0	0.1835	-0.7737	-0.6904	0.3123	0.0
$\mathbf{q}_1 \cdot \mathbf{q}_2 / \mathbf{q}_1^2$	0.0	-2247	2996	2247	-2996	0.0
$\mathbf{q}_2^2 (\mathbf{q}_1 \cdot \mathbf{q}_2) / \mathbf{q}_1^2$	0.0	80.66	-107.5	-80.66	107.5	0.0
$(\mathbf{q}_1 \cdot \mathbf{q}_2)^2 / \mathbf{q}_1^2$	0.0	8.571	-5.936	-5.352	12.49	0.0
$\mathbf{q}_1 \cdot \mathbf{q}_2 / \mathbf{q}_2^2$	0.0	0.0	3139	2354	0.0	0.0
$\mathbf{q}_1^2 (\mathbf{q}_1 \cdot \mathbf{q}_2) / \mathbf{q}_2^2$	0.0	0.0	-120.1	-90.08	0.0	0.0
$(\mathbf{q}_1 \cdot \mathbf{q}_2)^2 / \mathbf{q}_2^2$	0.0	0.0	-7.317	-6.512	0.0	0.0

because of the increased number of degrees of freedom (from 3 to 6 in comparison to $\Gamma^{(3)}$), to decide which datapoints and fit functions to use.

Approximations for $\Gamma_{IJKL}^{(4)}$ that can be used in deriving new phase separation models, must be derived in such a way that the combined $\Gamma^{(4)}$ is positive in the entire frequency domain. This approach does not contradict the conditions necessary for a sufficient description of phase separation and may well be a very practical solution.

A practical approximation for the trilinear term might be a simple factorization of the following form:

$$\begin{aligned}
& \nabla^2 \int_{V^3} \Gamma_{IJK}^{(4)}(\mathbf{r} - \mathbf{r}_1, \mathbf{r} - \mathbf{r}_2, \mathbf{r} - \mathbf{r}_3) \\
& \quad \times \tilde{\rho}_J(\mathbf{r}_1) \tilde{\rho}_K(\mathbf{r}_2) \tilde{\rho}_L(\mathbf{r}_3) d\mathbf{r}_1 d\mathbf{r}_2 d\mathbf{r}_3 \\
& \quad \approx c_{0IJKL} \nabla^2 \tilde{\rho}_J(\mathbf{r}) \tilde{\rho}_K(\mathbf{r}) \tilde{\rho}_L(\mathbf{r}) \\
& \quad + c_{1IJKL} \nabla^2 z_I(\mathbf{r}) z_J(\mathbf{r}) z_K(\mathbf{r}). \quad (42)
\end{aligned}$$

The first term replaces $\Gamma_{IJK}^{(4)}$ by its average in the nonsingular domain, and the second term is added to capture some of the complex singular behavior of $\Gamma_{IJKL}^{(4)}$.

VI. DISCUSSION AND CONCLUSIONS

The first question we must ask ourselves is whether the extensive mathematical analysis is really necessary to describe the dynamics of phase separation, or if a simple phenomenological model can be used just as well. We find that if we restrict ourselves to the basic physics of the problem and concentrate on the behaviors on a coarse-grained length scale (e.g., polymer coil size), the simplified phenomenological approaches outlined in the Introduction are sufficient. However, phase separation is in principle a process on

multiple-length scales. The second order vertex coefficient clearly shows that we must try to account for both density fluctuations on the polymer coil size length scale as well as for monomer-scale gradients in the interfacial regions between domains. The latter behavior is especially important in the strong segregation limit and for the irregular metastable structures in our simulations, where the density spectrum becomes broad. Hence, for the description of the physics of the complete multiple length-scale problem we really need the full analysis.

Next, we ask ourselves if the expansion approach provides an accurate and fast dynamical simulation. We recall from the Introduction that there are three prerequisites for the practical applicability of the fourth order expansion: (i) The expansion must be sufficient to guarantee phase separation, i.e., the fourth-order contribution must be positive, (ii) it must take the molecular details of the chain molecules into account, and (iii) it must lead to faster numerical algorithms. We have shown that even for a simple linear copolymer melt the fourth-order vertex coefficient as calculated in the present paper, is negative for some wave vectors. In a study of the relative stability of ordered phases in order to derive a mean-field phase diagram, this need not be consequential, depending on the lattice vectors that are considered in the analysis. If the lattice vectors are in the negative part of the frequency domain, the ordered phase is unstable for this particular approximation. If the lattice vectors are in the positive part of the frequency domain, the ordered phase is stable for this particular approximation. However, in a dynamics simulation the system is in principle free to choose its ‘‘own’’ preferred mesophase structure, which may have a very widespread density spectrum. In that case, a negative fourth-order contribution in the free energy may lead to amplification of

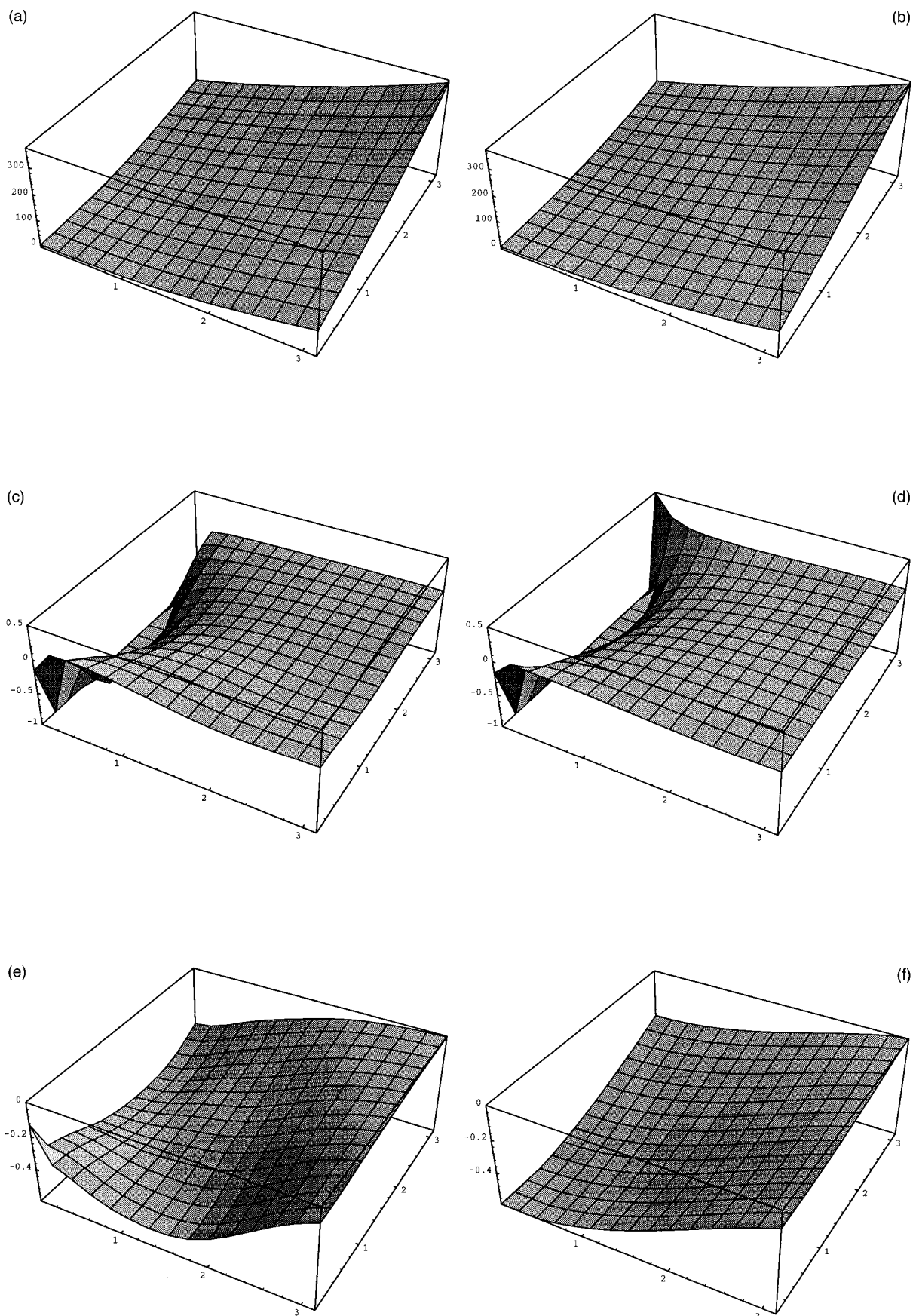


FIG. 5. $(\mathbf{q}_1 + \mathbf{q}_2)^2 \Gamma^{(3)}$ for A_8B_6 as a function of x and y . (a) Analytical result $(\mathbf{q}_1 + \mathbf{q}_2)^2 \Gamma_{AAA}^{(3)}$, $\mathbf{q}_1 \cdot \mathbf{q}_2 > 0$, $\mathbf{q}_1 = x(1,1,1)'$, $\mathbf{q}_2 = y(1,1,1)'$. (b) Fitted result $(\mathbf{q}_1 + \mathbf{q}_2)^2 \Gamma_{AAA}^{(3)}$, $\mathbf{q}_1 \cdot \mathbf{q}_2 > 0$. (c) Analytical result $(\mathbf{q}_1 + \mathbf{q}_2)^2 \Gamma_{AAB}^{(3)}$, $\mathbf{q}_1 \cdot \mathbf{q}_2 < 0$, $\mathbf{q}_1 = x(-1,0,1)'$, $\mathbf{q}_2 = y(1,1,-1)'$. (d) Fitted result $(\mathbf{q}_1 + \mathbf{q}_2)^2 \Gamma_{AAB}^{(3)}$, $\mathbf{q}_1 \cdot \mathbf{q}_2 < 0$. (e) Analytical result $(\mathbf{q}_1 + \mathbf{q}_2)^2 \Gamma_{ABB}^{(3)}$, $\mathbf{q}_1 \cdot \mathbf{q}_2 = 0$, $\mathbf{q}_1 = x(1,0,1)'$, $\mathbf{q}_2 = y(0,1,0)'$. (f) Fitted result $(\mathbf{q}_1 + \mathbf{q}_2)^2 \Gamma_{ABB}^{(3)}$, $\mathbf{q}_1 \cdot \mathbf{q}_2 = 0$.

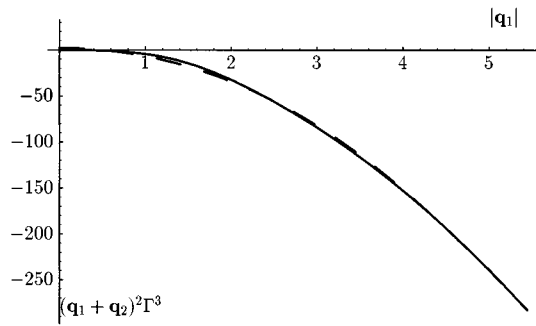


FIG. 6. Analytical (—) and fitted (---) $(\mathbf{q}_1 + \mathbf{q}_2)^2 \Gamma^{(3)}(\mathbf{q}_1, \mathbf{q}_2)$ for A_8B_6 as a function of $|\mathbf{q}_1|$ where $\mathbf{q}_1 = \mathbf{q}_2$.

completely artificial structures. Hence, we must conclude that the fourth-order expansion is not sufficient for dynamical simulations.

There are some practical difficulties in taking molecular detail into account. In principle the vertex coefficients can be calculated for any architecture (e.g., branched or combcopolymers) and chain composition.³⁵ However, the analytical formulas for the vertex coefficients become very complex unless the chain has a very high symmetry (such as a block copolymer). Their complexity makes the analytical formulas rather impractical to use unless severe simplifications are made.

We are not yet conclusive about the increased speed of the numerical calculations if we employ the fourth-order expansion. We must first obtain a free energy expansion that guarantees phase separation; either by extending the expansion to sixth order or by employing a phenomenological (symmetrized) approximation of the fourth-order vertex coefficient. On the other hand, the gradient expansion shows that in direct space the bilinear term becomes more compact than the linear term, and this is rather favorable from a computational point of view.

Returning to the phenomenological free energy models for incompressible systems outlined in the Introduction, our expansion for the bilinear term may perhaps point to an entirely new class of simplified phase-separation models for bicontinuous systems. It is known that asymmetric chains may lead to bicontinuous phases when the interactions are not too strong.^{19,31–33,36} From the data in Table I, we see that in case of the asymmetric chain all cross terms have extra inner-product terms $\mathbf{q}_1 \cdot \mathbf{q}_2$ and variants thereof, which are absent in the pure coefficients $\Gamma_{AAA}^{(3)}$ and $\Gamma_{BBB}^{(3)}$. From symmetry considerations, we expect that the inner-products are also important for the combined vertex coefficient $\Gamma^{(3)}$ in the incompressible system. For example, if we functionally integrate the term containing the $\mathbf{q}_1 \cdot \mathbf{q}_2$ fitfunction over the order parameter, we find the integral

$$F_{bc} = \frac{c}{3} \int_V \phi \nabla^2 \phi^2 d\mathbf{r}, \quad (43)$$

which could provide a first order approximation for bicontinuity in simplified phenomenological models. Further work to verify the conjecture is in progress.

ACKNOWLEDGMENTS

The work described in this paper was performed as part of the CAESAR project (Clusters of Computationally Intensive Applications for Engineering Design and Simulation on Scalable Parallel Architectures) which is funded under contract ESPRIT EP8328 of the European Community. The project is a collaboration between the British Aerospace (prime partner), DASA, Odense Steel Shipyard and BASF. We are thankful for the support by the European Community. We would also like to thank D. Andelman for stimulating discussions and Y. Gurovich for kindly providing us with some unpublished results.

APPENDIX A: *n*-BODY CORRELATORS

The Fourier forms of the *n*-body correlators read

$$G_{IJ}^{(2)}(\mathbf{q}) = \frac{n}{V} \sum_{i=1}^N \sum_{j=1}^N \delta_{iI}^K \delta_{jJ}^K \omega^{|i-j|}, \quad (A1)$$

$$G_{IJK}^{(3)}(\mathbf{q}_1, \mathbf{q}_2) = \frac{n}{V} \sum_{i=1}^N \sum_{j=1}^N \sum_{k=1}^N \delta_{iI}^K \delta_{jJ}^K \delta_{kK}^K f_{ijk}(\mathbf{q}_1, \mathbf{q}_2), \quad (A2)$$

$$G_{IJKL}^{(4)}(\mathbf{q}_1, \mathbf{q}_2, \mathbf{q}_3) = \frac{n}{V} \sum_{i=1}^N \sum_{j=1}^N \sum_{k=1}^N \sum_{l=1}^N \delta_{iI}^K \delta_{jJ}^K \delta_{kK}^K \times \delta_{lL}^K g_{ijkl}(\mathbf{q}_1, \mathbf{q}_2, \mathbf{q}_3), \quad (A3)$$

$$f_{ijk}(\mathbf{q}_1, \mathbf{q}_2) = \begin{cases} \omega_{12}^{|i-j|} \omega_2^{|k-j|} & \text{if } i \leq j \leq k \text{ or } k \leq j \leq i \\ \omega_{12}^{|k-i|} \omega_1^{|k-j|} & \text{if } i \leq k \leq j \text{ or } j \leq k \leq i, \\ \omega_1^{|i-j|} \omega_2^{|k-i|} & \text{if } j \leq i \leq k \text{ or } k \leq i \leq j \end{cases} \quad (A4)$$

$$g_{ijkl}(\mathbf{q}_1, \mathbf{q}_2, \mathbf{q}_3) = \begin{cases} \omega_{123}^{|i-j|} \omega_{23}^{|k-j|} \omega_3^{|k-l|} & \text{if } i \leq j \leq k \leq l \text{ or } l \leq k \leq j \leq i \\ \omega_{123}^{|i-j|} \omega_{23}^{|l-j|} \omega_2^{|k-l|} & \text{if } i \leq j \leq l \leq k \text{ or } k \leq l \leq j \leq i \\ \omega_{123}^{|k-i|} \omega_{13}^{|k-j|} \omega_3^{|l-j|} & \text{if } i \leq k \leq j \leq l \text{ or } l \leq j \leq k \leq i \\ \omega_{123}^{|k-i|} \omega_{13}^{|k-l|} \omega_1^{|l-j|} & \text{if } i \leq k \leq l \leq j \text{ or } j \leq l \leq k \leq i \\ \omega_{123}^{|l-i|} \omega_{12}^{|j-l|} \omega_2^{|k-j|} & \text{if } i \leq l \leq j \leq k \text{ or } k \leq j \leq l \leq i \\ \omega_{123}^{|l-i|} \omega_{12}^{|k-l|} \omega_1^{|k-j|} & \text{if } i \leq l \leq k \leq j \text{ or } j \leq k \leq l \leq i \\ \omega_1^{|i-j|} \omega_{23}^{|i-k|} \omega_3^{|k-l|} & \text{if } j \leq i \leq k \leq l \text{ or } l \leq k \leq i \leq j \\ \omega_1^{|i-j|} \omega_{23}^{|i-l|} \omega_2^{|k-l|} & \text{if } j \leq i \leq l \leq k \text{ or } k \leq l \leq i \leq j \\ \omega_2^{|i-k|} \omega_{13}^{|i-l|} \omega_3^{|j-l|} & \text{if } l \leq j \leq i \leq k \text{ or } k \leq i \leq j \leq l \\ \omega_2^{|k-j|} \omega_{12}^{|i-l|} \omega_3^{|i-l|} & \text{if } l \leq i \leq j \leq k \text{ or } k \leq j \leq i \leq l \\ \omega_1^{|j-l|} \omega_{13}^{|l-i|} \omega_2^{|i-k|} & \text{if } j \leq l \leq i \leq k \text{ or } k \leq i \leq l \leq j \\ \omega_1^{|j-k|} \omega_{12}^{|i-k|} \omega_3^{|i-l|} & \text{if } j \leq k \leq i \leq l \text{ or } l \leq i \leq k \leq j \end{cases} \quad (A5)$$

$$\omega = \exp\left(-\frac{a^2 \mathbf{q}^2}{6}\right), \quad (\text{A6})$$

$$\omega_i = \exp\left(-\frac{a^2 \mathbf{q}_i^2}{6}\right), \quad (\text{A7})$$

$$\omega_{ij} = \exp\left[-\frac{a^2 (\mathbf{q}_i + \mathbf{q}_j)^2}{6}\right], \quad (\text{A8})$$

$$\omega_{ijk} = \exp\left[-\frac{a^2 (\mathbf{q}_i + \mathbf{q}_j + \mathbf{q}_k)^2}{6}\right]. \quad (\text{A9})$$

In the calculations we have omitted an unimportant bead volume parameter and have set $n/V = 1/N$.

APPENDIX B: ONE-STEP ITERATION TECHNIQUE AND SYMMETRIZATION PROCEDURE

For a one-dimensional function the one-step iteration technique leads to very simple expressions. Suppose the one-dimensional functions y and x are expanded to third order:

$$y = ax + bx^2 + cx^3, \quad (\text{B1})$$

$$x = dy + ey^2 + fy^3. \quad (\text{B2})$$

We can relate the expansion coefficients of x and y by inserting the expression for x in y and equating powers of y to third order. This leads to

$$1 = ad, \quad (\text{B3})$$

$$0 = ae + bd^2, \quad (\text{B3})$$

$$0 = af + 2bde + cd^3,$$

if all coefficients commute. These relations are unique. For a functional expansion to third order however, the relations need no longer all be unique. This can be illustrated by the one-order parameter density and external potential expansions. We now have the following expansions in Fourier space [cf. Eqs. (22) and (24)]:

$$\begin{aligned} \tilde{\rho}(\mathbf{q}) = & -\beta G^{(2)}(\mathbf{q})U(\mathbf{q}) + \frac{\beta^2}{2} \int_V G^{(3)}(\mathbf{q}-\mathbf{q}_2, \mathbf{q}_2) \\ & \times U(\mathbf{q}-\mathbf{q}_2)U(\mathbf{q}_2)d\mathbf{q}_2 \\ & - \frac{\beta^3}{6} \int_V \int_V G^{(4)}(\mathbf{q}-\mathbf{q}_2-\mathbf{q}_3, \mathbf{q}_2, \mathbf{q}_3) \\ & \times U(\mathbf{q}-\mathbf{q}_2-\mathbf{q}_3)U(\mathbf{q}_2)U(\mathbf{q}_3)d\mathbf{q}_2 d\mathbf{q}_3, \end{aligned} \quad (\text{B4})$$

$$\begin{aligned} U(\mathbf{q}) = & -\frac{1}{\beta} \Gamma^{(2)}(\mathbf{q})\tilde{\rho}(\mathbf{q}) - \frac{1}{2\beta} \int_V \Gamma^{(3)}(\mathbf{q}-\mathbf{q}_2, \mathbf{q}_2) \\ & \times \tilde{\rho}(\mathbf{q}-\mathbf{q}_2)\tilde{\rho}(\mathbf{q}_2)d\mathbf{q}_2 - \frac{1}{6\beta} \int_V \int_V \Gamma^{(4)}(\mathbf{q}-\mathbf{q}_2-\mathbf{q}_3, \\ & \mathbf{q}_2, \mathbf{q}_3)\tilde{\rho}(\mathbf{q}-\mathbf{q}_2-\mathbf{q}_3)\tilde{\rho}(\mathbf{q}_2)\tilde{\rho}(\mathbf{q}_3)d\mathbf{q}_2 d\mathbf{q}_3. \end{aligned} \quad (\text{B5})$$

We now insert the expression for $U(\mathbf{q})$ in the expression for $\tilde{\rho}(\mathbf{q})$ and equate integrals of the same power in $\tilde{\rho}$. This yields

$$\tilde{\rho}(\mathbf{q}) = G^{(2)}(\mathbf{q})\Gamma^{(2)}(\mathbf{q})\tilde{\rho}(\mathbf{q}), \quad (\text{B6})$$

$$\begin{aligned} 0 = & \int_V [G^{(2)}(\mathbf{q})\Gamma^{(3)}(\mathbf{q}-\mathbf{q}_2, \mathbf{q}_2) + G^{(3)}(\mathbf{q}-\mathbf{q}_2, \mathbf{q}_2) \\ & \times \Gamma^{(2)}(\mathbf{q}-\mathbf{q}_2)\Gamma^{(2)}(\mathbf{q}_2)]\tilde{\rho}(\mathbf{q}-\mathbf{q}_2)\tilde{\rho}(\mathbf{q}_2)d\mathbf{q}_2, \end{aligned} \quad (\text{B7})$$

$$\begin{aligned} 0 = & \int_V \int_V [G^{(2)}(\mathbf{q})\Gamma^{(4)}(\mathbf{q}-\mathbf{q}_2-\mathbf{q}_3, \mathbf{q}_2, \mathbf{q}_3) + G^{(4)}(\mathbf{q}-\mathbf{q}_2 \\ & -\mathbf{q}_3, \mathbf{q}_2, \mathbf{q}_3)\Gamma^{(2)}(\mathbf{q}-\mathbf{q}_2-\mathbf{q}_3)\Gamma^{(2)}(\mathbf{q}_2)\Gamma^{(2)}(\mathbf{q}_3) \\ & + \frac{3}{2} G^{(3)}(\mathbf{q}-\mathbf{q}_2-\mathbf{q}_3, \mathbf{q}_2+\mathbf{q}_3)\Gamma^{(2)}(\mathbf{q}-\mathbf{q}_2-\mathbf{q}_3)\Gamma^{(3)} \\ & \times (\mathbf{q}_2, \mathbf{q}_3) + \frac{3}{2} G^{(3)}(\mathbf{q}-\mathbf{q}_3, \mathbf{q}_3)\Gamma^{(3)}(\mathbf{q}-\mathbf{q}_2-\mathbf{q}_3, \mathbf{q}_2) \\ & \times \Gamma^{(2)}(\mathbf{q}_3)]\tilde{\rho}(\mathbf{q}-\mathbf{q}_2-\mathbf{q}_3)\tilde{\rho}(\mathbf{q}_2)\tilde{\rho}(\mathbf{q}_3)d\mathbf{q}_2 d\mathbf{q}_3. \end{aligned} \quad (\text{B8})$$

Sufficient conditions for these integral equations to hold are [cf. Eqs. (26) and (B3)]

$$1 = G^{(2)}(\mathbf{q})\Gamma^{(2)}(\mathbf{q}), \quad (\text{B9})$$

$$\begin{aligned} 0 = & G^{(2)}(\mathbf{q}_1+\mathbf{q}_2)\Gamma^{(3)}(\mathbf{q}_1, \mathbf{q}_2) + G^{(3)}(\mathbf{q}_1, \mathbf{q}_2)\Gamma^{(2)}(\mathbf{q}_1) \\ & \times \Gamma^{(2)}(\mathbf{q}_2), \end{aligned} \quad (\text{B10})$$

$$\begin{aligned} 0 = & G^{(2)}(\mathbf{q}_1+\mathbf{q}_2+\mathbf{q}_3)\Gamma^{(4)}(\mathbf{q}_1, \mathbf{q}_2, \mathbf{q}_3) \\ & + G^{(4)}(\mathbf{q}_1, \mathbf{q}_2, \mathbf{q}_3)\Gamma^{(2)}(\mathbf{q}_1)\Gamma^{(2)}(\mathbf{q}_2)\Gamma^{(2)}(\mathbf{q}_3) \\ & + \frac{3}{2} G^{(3)}(\mathbf{q}_1, \mathbf{q}_2+\mathbf{q}_3)\Gamma^{(2)}(\mathbf{q}_1)\Gamma^{(3)}(\mathbf{q}_2, \mathbf{q}_3) \\ & + \frac{3}{2} G^{(3)}(\mathbf{q}_1+\mathbf{q}_2, \mathbf{q}_3)\Gamma^{(3)}(\mathbf{q}_1, \mathbf{q}_2)\Gamma^{(2)}(\mathbf{q}_3). \end{aligned} \quad (\text{B11})$$

Now, the fourth-order relationship is not unique. In any of the integral Eqs. (B6)–(B8) we can transform the integration variables before equating the integral kernels. For the second- and third-order relationships, this does not lead to different relationships, but it does change the fourth-order relationship. Since the integral Eq. (B8) is of the form

$$\begin{aligned} 0 = & \int_V \int_V \text{kernel}(\mathbf{q}-\mathbf{q}_2-\mathbf{q}_3, \mathbf{q}_2, \mathbf{q}_3)\tilde{\rho}(\mathbf{q}-\mathbf{q}_2-\mathbf{q}_3) \\ & \times \tilde{\rho}(\mathbf{q}_2)\tilde{\rho}(\mathbf{q}_3)d\mathbf{q}_2 d\mathbf{q}_3, \end{aligned} \quad (\text{B12})$$

we can employ either of the following variable transforms for another sufficient relation:

$$\mathbf{q}_3 := \tilde{\mathbf{q}}_2, \quad \mathbf{q}_2 := \tilde{\mathbf{q}}_3, \quad (\text{B13})$$

$$\mathbf{q}_2 := \mathbf{q} - \tilde{\mathbf{q}}_2 - \mathbf{q}_3, \quad (\text{B14})$$

$$\mathbf{q}_2 := \tilde{\mathbf{q}}_3, \quad \mathbf{q}_3 := \mathbf{q} - \tilde{\mathbf{q}}_2 - \tilde{\mathbf{q}}_3, \quad (\text{B15})$$

$$\mathbf{q}_3 := \tilde{\mathbf{q}}_2, \quad \mathbf{q}_2 := \mathbf{q} - \tilde{\mathbf{q}}_2 - \tilde{\mathbf{q}}_3, \quad (\text{B16})$$

$$\mathbf{q}_3 := \mathbf{q} - \mathbf{q}_2 - \tilde{\mathbf{q}}_3. \quad (\text{B17})$$

If we average the six resulting relationships and employ the lower order symmetries for $G^{(3)}$ and $G^{(4)}$ we arrive at the following relationship for $\Gamma^{(4)}$ in a one-order parameter system in terms of n -body correlators:

$$\begin{aligned}
 0 = & G^{(2)}(\mathbf{q}_1 + \mathbf{q}_2 + \mathbf{q}_3)\Gamma^{(4)}(\mathbf{q}_1, \mathbf{q}_2, \mathbf{q}_3) + G^{(4)} \\
 & \times (\mathbf{q}_1, \mathbf{q}_2, \mathbf{q}_3)\Gamma^{(2)}(\mathbf{q}_1)\Gamma^{(2)}(\mathbf{q}_2)\Gamma^{(2)}(\mathbf{q}_3) + G^{(3)}(\mathbf{q}_1, \mathbf{q}_2 \\
 & + \mathbf{q}_3)\Gamma^{(2)}(\mathbf{q}_1)\Gamma^{(3)}(\mathbf{q}_2, \mathbf{q}_3) + G^{(3)}(\mathbf{q}_1 + \mathbf{q}_2, \mathbf{q}_3) \\
 & \times \Gamma^{(3)}(\mathbf{q}_1, \mathbf{q}_2)\Gamma^{(2)}(\mathbf{q}_3) + G^{(3)}(\mathbf{q}_1 + \mathbf{q}_3, \mathbf{q}_2) \\
 & \times \Gamma^{(3)}(\mathbf{q}_1, \mathbf{q}_3)\Gamma^{(2)}(\mathbf{q}_2). \tag{B18}
 \end{aligned}$$

This automatically yields a symmetric $\Gamma^{(4)}$, which is directly comparable to Γ_4 of Leibler.²⁰ Hence, if we use the different representations of the fourth-order integral equation, we simply symmetrize the fourth-order relationship. Notice however that the physical symmetries of $\Gamma^{(4)}$ do *not* automatically follow from the one-step iteration technique. In principle we could use a similar procedure to symmetrize $\Gamma^{(4)}$ in a multiple-order parameter system. Since the lower order symmetries are now much more complex ($G^{(4)}$ is a 16-element matrix in a binary system) the symmetrized expression for $\Gamma^{(4)}$ can not easily be simplified and a very unwieldy and hard to calculate expression remains.

¹O. T. Valls and J. E. Farrell, Phys. Rev. E **47**, R36 (1993).

²T. Kawakatsu, K. Kawasaki, M. Furusaka, H. Okabayashi, and T. Kanaya, J. Chem. Phys. **99**, 8200 (1993).

³A. Shinozaki and Y. Oono, Phys. Rev. E **48**, 2622 (1993).

⁴M. C. Cross and P. C. Hohenberg, Rev. Mod. Phys. **65**, 851 (1993).

⁵B. Schmittmann and R. K. P. Zia, *Phase Transitions and Critical Phenomena*, edited by C. Domb and J. Lebowitz (Academic, London, 1994).

⁶B. A. C. Van Vlimmeren and J. G. E. M. Fraaije, Comp. Phys. Commun. **99**, 21 (1996).

⁷C. W. Gardiner, *Handbook of Stochastic Methods* (Springer, Berlin, 1990).

⁸H. Risken, *The Fokker-Planck Equation* (Springer, Berlin, 1989).

⁹M. Seul and D. Andelman, Science **267**, 476 (1995).

¹⁰Y. Oono and Y. Shiwa, Mod. Phys. Lett. B **1**, 49 (1987).

¹¹Y. Oono and M. Bahiana, Phys. Rev. Lett. **61**, 1109 (1988).

¹²F. Liu and N. Goldenfeld, Phys. Rev. A **39**, 4805 (1989).

¹³A. Chakrabarti, R. Toral, and J. D. Gunton, Phys. Rev. E **47**, 3025 (1993).

¹⁴G. Brown and A. Chakrabarti, J. Chem. Phys. **101**, 3310 (1994).

¹⁵Y. Oono and S. Puri, Phys. Rev. Lett. **58**, 836 (1987).

¹⁶Y. Oono and S. Puri, Phys. Rev. A **38**, 434 (1988).

¹⁷M. Bahiana and Y. Oono, Phys. Rev. A **41**, 6763 (1990).

¹⁸N. M. Maurits, P. Altevogt, O. A. Evers, and J. G. E. M. Fraaije, Comp. Polym. Sci. **6**, 1 (1996).

¹⁹J. G. E. M. Fraaije, B. A. C. van Vlimmeren, N. M. Maurits, M. Postma, O. A. Evers, C. Hoffmann, P. Altevogt, and G. Goldbeck-Wood, J. Chem. Phys. **106**, 4260 (1997).

²⁰L. Leibler, Macromolecules **13**, 1602 (1980).

²¹J. Melenkevitz and M. Muthukumar, Macromolecules **24**, 4199 (1991).

²²A. M. Mayes, M. Olvera de La Cruz, and W. E. McMullen, Macromolecules **26**, 4050 (1993).

²³W. E. McMullen, Macromolecules **26**, 1027 (1993).

²⁴M. Doi and S. F. Edwards, *The Theory of Polymer Dynamics* (Clarendon, Oxford, 1986).

²⁵P.-G. de Gennes, *Scaling Concepts in Polymer Physics* (Cornell University Press, Ithaca, NY, 1979).

²⁶N. David Mermin, Phys. Rev. **137**, 1441 (1965).

²⁷R. A. Horn and C. R. Johnson, *Topics in Matrix Analysis* (Cambridge University Press, Cambridge, UK, 1991).

²⁸P. M. Chaikin and T. C. Lubensky, *Principles of Condensed Matter Physics* (Cambridge University Press, Cambridge, UK, 1995).

²⁹E. Gurovich, L. Leibler, and J. Prost, (unpublished).

³⁰A. M. Mayes and M. Olvera de La Cruz, Macromolecules **24**, 3975 (1991).

³¹M. W. Matsen and F. S. Bates, Macromolecules **29**, 1091 (1996).

³²M. W. Matsen and M. Schick, Phys. Rev. Lett. **72**, 2660 (1994).

³³M. W. Matsen and M. Schick, Macromolecules **27**, 7157 (1994).

³⁴J. G. E. M. Fraaije, J. Chem. Phys. **99**, 9202 (1993).

³⁵A. V. Dobrynin and I. Ya. Erukhimovich, Macromolecules **26**, 276 (1993).

³⁶F. S. Bates, M. F. Schulz, A. K. Khandpur, S. Forster, and J. H. Rosedale, Faraday Discuss. **98**, 7 (1994).